# Changes in Column Ozone Correlated with the Stratospheric EP Flux

**William J. RANDEL, Fei WU**

*National Center for Atmospheric Research, Boulder, CO, USA*

**and**

**Richard STOLARSKI**

*NASA Goddard Space Flight Center, Greenbelt, MD, USA*

*(Manuscript received 4 June 2001, in revised form 18 March 2002)*

## Abstract

Variability in planetary wave forcing from the troposphere to the stratosphere is reflected in changes in ozone transport, due to fluctuations in the stratospheric Brewer-Dobson circulation and eddy mixing. This work examines the space-time patterns of correlations between column ozone tendency and planetary wave Eliassen-Palm (EP) flux into the lower stratosphere, using monthly mean data for 1979–2000. Strong correlations are found during winter–spring in both hemispheres, with out-of-phase ozone changes between the tropics and middle-high latitudes. Springtime polar ozone is strongly influenced by wave forcing in both the Arctic and Antarctic. The ozone tendency–wave forcing correlations are combined with observed variations in EP flux to estimate the dynamic contribution to decadal-scale NH ozone trends. These calculations suggest that interannual changes in EP flux contribute ~20–30% of the observed trends in column ozone over 35–60°N during the past two decades.

## 1. Introduction

Stratospheric ozone is strongly influenced by meteorological variability on both short and long time scales. This is evidenced by the observed strong correlations between ozone and a wide range of meteorological parameters, such as tropopause height (Schubert and Muntenau 1988; Steinbrecht et al. 1998), lower stratospheric temperature (Randel and Cobb 1994), and potential vorticity (Allaart et al. 1993; Hood et al. 1999). The dominant role of dynamics for extratropical ozone is also emphasized in the modeling studies of Hadjinicolaou et al. (1997, 2002) and Kinnersley and Tung (1998). Ziemke et al. (1997) have investigated a number of dynamical proxies which are empirically correlated to column ozone. The use of such dynamical proxies is central to accurate characterization of dynamic ozone variability. This dynamical attribution is most straightforward for (fast) synoptic-scale variability, but becomes complicated for interannual or decadal-scale changes. This is because on long time scales ozone changes can influence the dynamical field (such as lower stratospheric temperature via radiative effects), and hence a 'clean' isolation of the effect of dynamics is not possible.

The recent work of Fusco and Salby (1999) has suggested a further dynamical proxy which exhibits strong correlation with column ozone. They show that variations in planetary wave activity entering the lower stratosphere (specifically, the vertical component of the Eliassen-Palm or EP flux ($F_z$)) are coherent with ten-

Corresponding author: William J. Randel, National Center for Atmospheric Research, Boulder, CO 80307, USA.
E-mail: randel@ucar.edu

dencies in column ozone. The mechanism for this correlation is that variations in the stratospheric EP flux divergence force commensurate changes in the stratospheric mean meridional (Brewer-Dobson) circulation, which in turn influence ozone transport. The EP flux divergence in the stratosphere is primarily determined by the amount of flux crossing the tropopause, so $F_z$ in the lower stratosphere may be a useful proxy for forcing of the stratospheric circulation. Evidence for this mechanism is seen in the latitudinal structure of the ozone tendency correlations, which are out-of-phase between the tropics and high latitudes (reflecting the overturning Brewer-Dobson circulation). This global-scale latitudinal see-saw is also apparent in stratospheric temperature changes during planetary wave events (first noted in satellite observations by Fritz and Soules 1972), and first documented in satellite ozone measurements in Randel (1993). Smith (1995) has accurately simulated these global stratospheric variations, using an idealized three-dimensional model forced by transient tropospheric wave events.

The relation between zonal mean ozone tendency and dynamic variability can be quantified by the transformed Eulerian-mean (TEM) continuity equation (Andrews et al. 1987, Eq. 9.4.13):

$$\frac{\partial \bar{\chi}}{\partial t} = -\overline{v^*}\bar{\chi}_y - \overline{w^*}\bar{\chi}_z + \nabla \cdot \vec{M} + \bar{S}. \qquad (1)$$

Here $\bar{\chi}$ is the zonal mean mixing ratio, $(\overline{v^*}, \overline{w^*})$ are components of the mean meridional circulation, $\nabla \cdot \vec{M}$ is an eddy transport term, and $\bar{S}$ is a chemical source/sink term. Variations in planetary wave EP flux entering the lower stratosphere are associated with changes in $(\overline{v^*}, \overline{w^*})$ (e.g., Haynes et al. 1991), and also result in fluctuating eddy transports ($\nabla \cdot \vec{M}$). Both mean and eddy transports are important in general (Mahlman et al. 1986; Randel et al. 1994), and column ozone has the further complication of being the result of transport effects over a deep layer of the stratosphere (or this vertical integration can be a simplification if competing effects cancel when integrated in height). Furthermore, seasonal variations in radiative heating also drive some component of the $(\overline{v^*}, \overline{w^*})$ circulation (Garcia 1987) so that not all of the ozone transport is necessarily related to tropospheric wave forcing. Given this overall complexity, it is somewhat surprising that observations show strong correlations between column ozone and lower stratospheric EP fluxes. However, this empirical result makes the EP flux an attractive proxy for isolating dynamic variability in column ozone. Newman et al. (2001) find strong correlations between lower stratospheric EP flux and polar stratospheric temperatures, confirming its utility as a concise dynamical proxy. An additional advantage is that there should be relatively little direct feedback between ozone and planetary wave EP fluxes entering the lower stratosphere.

The relationship between midlatitude column ozone and lower stratospheric EP fluxes (quantified by the 100 mb eddy heat flux, $\overline{v'T'}$, as discussed below) is illustrated in Fig. 1, showing daily time series for two separate years (1980–1981 and 1987–1988). There is a systematic ozone increase during midwinter each year, approximately coincident with the seasonal maximum in EP fluxes. However, detailed comparisons between these two years shows substantially larger ozone increase dur-

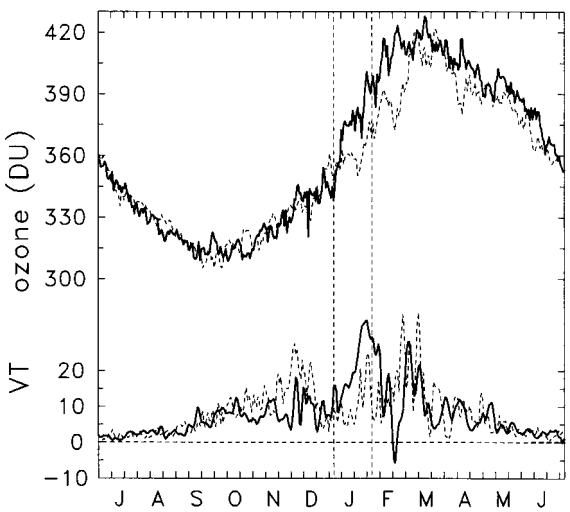


Fig. 1. Time series of daily column ozone at 50°N (top curves), together with daily $\overline{v'T'}$ in the lower stratosphere (lower curves). Results are shown for two years, contrasting 1980–1981 (dark line) and 1987–1988 (light, dashed line). The dashed vertical lines denote the month of January.

ing January 1981 than in January 1988, and this is associated with almost twice as much EP flux in January 1981. Much of this difference in EP fluxes is due to the stochastic nature of planetary wave variability, and these two years were chosen because of their extreme differences during January. However, the apparent impact on midlatitude ozone tendencies is dramatic, and shows the sensitivity to variability in planetary wave forcing.

The objective of this study is to quantify the space-time relationships between column ozone tendency and lower stratospheric EP flux, using an updated global record spanning 1979–2000. The spatial patterns of correlation are analyzed, together with their seasonal variation, and results are compared for NH and SH statistics (which show a high degree of similarity). These correlations demonstrate the importance of large-scale transport effects on ozone in the tropics, midlatitudes and polar regions. We furthermore quantify the effects of interannual changes in EP flux on decadal-scale ozone trends, based on integrating the ozone tendencies and isolating the wave forcing effects (quantified by regression). A key result is that changes in EP flux contribute a small but not inconsequential fraction (~20–30%) of observed decadal-scale 'trends' in ozone over NH midlatitudes.

## 2. Data and analyses

### 2.1 Ozone

The column ozone data studied here are derived from a combination of Total Ozone Mapping Spectrometer (TOMS) and Solar Backscatter Ultraviolet (SBUV and SBUV/2) satellite data sets spanning November 1978–July 2000. These include measurements from six individual satellite instruments, which have been combined to provide nearly continuous global coverage. An external calibration adjustment has been applied to each satellite data set (derived from temporal overlaps) to obtain an internally consistent global record. Details of the merged data set are discussed in Stolarski et al. (2002), and the data are available at http://code916.gsfc.nasa.gov/Data_services/merged/. In addition to the lack of measurements during polar night (characteristic of TOMS and SBUV sampling), there are a few extended periods of missing observations during 1993–1995, particularly at high latitudes (as seen in some of the plots below).

The original data set analyzed here are daily zonal means. Monthly averages are calculated simply as an average of all observations for each month, and deseasonalized anomalies are calculated by subtracting the mean seasonal cycle averaged over 1979–2000.

Calculation of monthly ozone tendencies (referred to throughout this paper as $\Delta O_3/\Delta t$) is based on simple differences between the ozone values on the first of each month, i.e., $\Delta O_3/\Delta t$ (January) = $O_3$ (February 1) – $O_3$ (January 1). This is equivalent to the monthly average of daily tendencies, and is temporally consistent with monthly mean sampling of the EP flux.

### 2.2 EP fluxes

A concise measure of the amount of planetary wave activity propagating into the lower stratosphere is given by the vertical component of EP flux, which in the quasi-geostrophic approximation is proportional to the zonally averaged eddy heat flux $\overline{v'T'}$ (e.g., Andrews et al. 1987, Eq. 3.5.6). While details of the ozone transport and mixing will depend on the fate of each particular wave event (i.e., propagation to low latitudes or focusing to the pole), to first approximation it is reasonable to expect the EP flux entering the lower stratosphere to be a useful dynamical proxy (Fusco and Salby 1999; Newman et al. 2001). We obtain estimates of $\overline{v'T'}$ from the NCEP/NCAR reanalyses (Kalnay et al. 1996), and calculate monthly means for the period January 1979–July 2000. We use $\overline{v'T'}$ at 100 mb, area averaged over 40–70° in each hemisphere, to provide reference time series for the ozone tendency correlations (a single value for each month). This 40–70° latitude range is where $\overline{v'T'}$ maximizes in each hemisphere; virtually identical results are obtained using averages over the entire hemisphere. A discussion of the uncertainty in $\overline{v'T'}$ statistics in the Northern Hemisphere can be found in Newman and Nash (2000); comparisons of individual monthly means from different meteorological analyses suggests an uncertainty of order ~15%. Somewhat larger differences are found comparing $\overline{v'T'}$ statistics in the data sparse Southern Hemisphere (as shown below in Fig. 16), particularly for long-

term variations, and in this paper we focus on decadal variability only in the NH.

As a note, it is important to appreciate that transience in lower stratospheric $\overline{v'T'}$ occurs primarily in the form of episodic wave events throughout winter and spring, with the individual events having a time scale of 1–2 weeks (see Fig. 1). While we choose an analysis here based on monthly means (for convenience and comparison to previous work), results for any particular month will depend on the timing of individual events, and this is one source of variability in these results. This is overcome somewhat by the use of a long record (22 years of statistics).

## 3. Climatology and variability of $\Delta O_3/\Delta t$

The fundamental question here is how much of the variability of $\Delta O_3/\Delta t$ is related to changes in $\overline{v'T'}$, so it is important to understand the variability of $\Delta O_3/\Delta t$ in the observed record. Figure 2 shows the monthly climatology of column ozone during 1979–2000, together with the climatological average ozone tendency field ($\Delta O_3/\Delta t$). Column ozone shows the well-known behavior of minima in the tropics and maxima in extratropics during the respective spring in each hemisphere (near the polar cap in the NH, and over the 40–60° 'collar' region in the SH). The extratropical seasonal cycle is reflected in the tendencies, with a build-up of ozone ($\Delta O_3/\Delta t > 0$) over NH extratropics during ~November–February, and over SH midlatitudes during ~May–September. This is presumably due to the transport of ozone from the tropics to high latitudes by the Brewer-Dobson circulation ($\overline{v^*}, \overline{w^*}$), plus large-scale eddy transports ($\nabla \cdot \vec{M}$ in Eq. 1), which maximize in each hemisphere during these months. Tropical ozone variations are furthermore consistent with this picture, as tropical minima occur during these periods of maximum transport (which is upward in the tropics, acting to decrease column ozone).

The actual year-to-year variability in $\Delta O_3/\Delta t$ over 40–50°N is shown in Fig. 3a. While the overall pattern is similar for each year (e.g., positive tendencies during November–February), there is substantial interannual variability (which translates to observed interannual changes in column ozone). Figure 3b shows a similar plot illustrating the variability

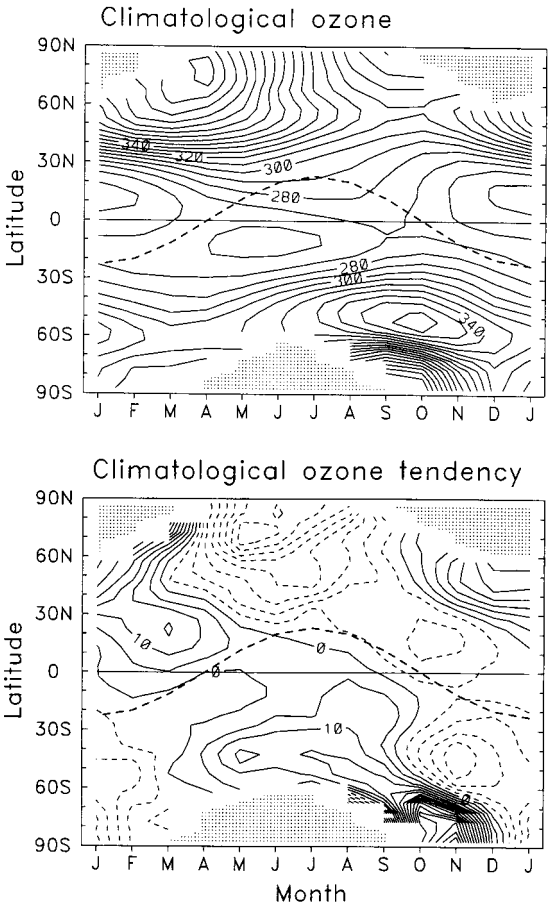


Fig. 2. Latitude-time plots of variations in column ozone (top, units of Dobson Units), and column ozone tendency $\Delta O_3/\Delta t$ (bottom, units of Dobson Units/month), derived from observations over 1979–2000. The heavy dashed line shows the sub-solar point.

of monthly mean lower stratospheric $\overline{v'T'}$ in the NH. Maximum wave activity is found in the NH during November–March, lagged approximately one month compared to the maximum $\Delta O_3/\Delta t$ at 40–50°N. Similar statistics are shown for the SH in Fig. 4. In the SH positive $\Delta O_3/\Delta t$ during ~May–September coincides with somewhat elevated wave activity, but the strong wave fluxes in SH spring (October–November) occur when $\Delta O_3/\Delta t$ is small or negative (suggesting predominant photochemical control for midlatitude ozone at this time).

An additional interesting feature in Figs. 3–4 is that ozone tendencies at midlatitudes have

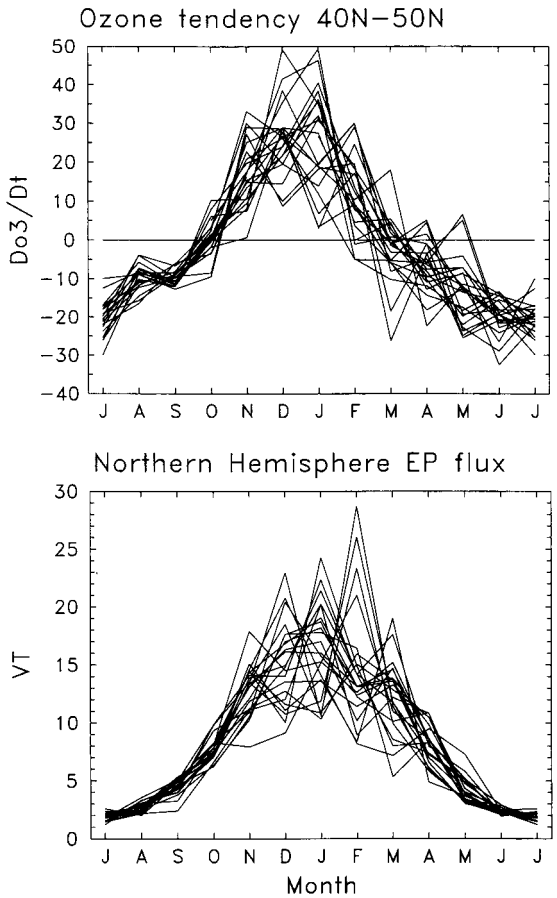


Fig. 3. (a) Time series of monthly column ozone tendency $\Delta O_3/\Delta t$ (DU/month) over 40–50°N, showing overlapping data for each year during 1979–2000. (b) Time series of monthly averaged 100 mb NH $\overline{v'T'}$ ($\mathrm{Kms}^{-1}$) for each year 1979–2000.

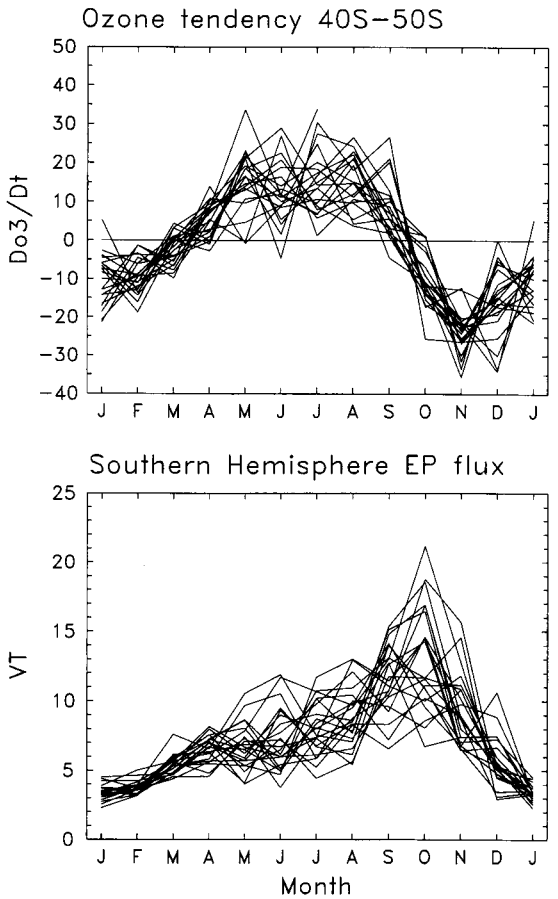


Fig. 4. Time series of monthly column ozone tendency (DU/month) and $\overline{v'T'}$ ($\mathrm{Kms}^{-1}$) for SH statistics over 1979–2000. The sign of $\overline{v'T'}$ (negative in the SH) is reversed, because the expression for EP flux contains a (negative) Coriolis parameter term.

substantial interannual variance throughout most of the year, even during times of minimum planetary wave activity (such as May–July at 40–50°N and January–February at 40–50°S). Part of this late spring-early summer ozone variability is likely due to photochemical relaxation, wherein years with large accumulation of winter–spring ozone experience subsequent stronger photochemical losses (as suggested in Fusco and Salby 1999, their Fig. 2). This relationship is confirmed by the scatter diagram in Fig. 5, showing a negative correlation at 40–50°N between ozone amount in April and ozone tendency ($\Delta O_3/\Delta t$) in May (i.e., large April ozone correlates with strong negative tendencies in May, and vice-versa). A regression fit of the midlatitude data in Fig. 5 to a relaxational form $\left(\Delta O_3/\Delta t = -\frac{1}{\tau}\cdot O_3\right)$ gives an approximate relaxational time scale $\tau \sim 1.5$ months; strong negative correlations are also found in the 60–90° polar cap in summer, with a somewhat longer inferred $\tau \sim 3$ months.

## 4. Correlations between $\Delta O_3/\Delta t$ and $\overline{v'T'}$

Monthly correlations between the reference time series $\overline{v'T'}$ in each hemisphere and $\Delta O_3/\Delta t$ as a function of latitude are shown in Fig. 6. Given 22 years of observations (1979–

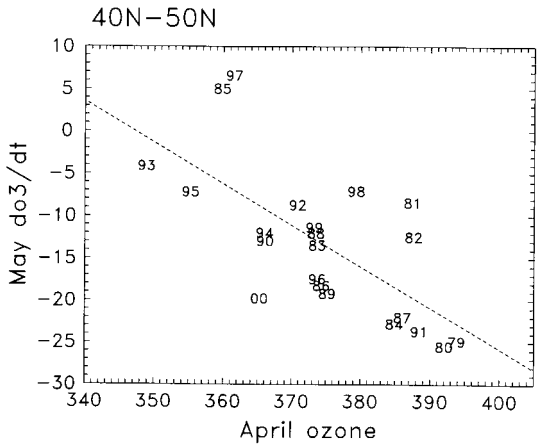


Fig. 5. Scatter diagram showing relationship between total ozone amount (DU) in April and ozone tendency (DU/month) in May, for statistics over 40–50°N. The numbers refer to the individual years, i.e., 79 = 1979. The slope of the regression fit (dashed line) corresponds to a photochemical relaxational time scale of ~1.5 months.

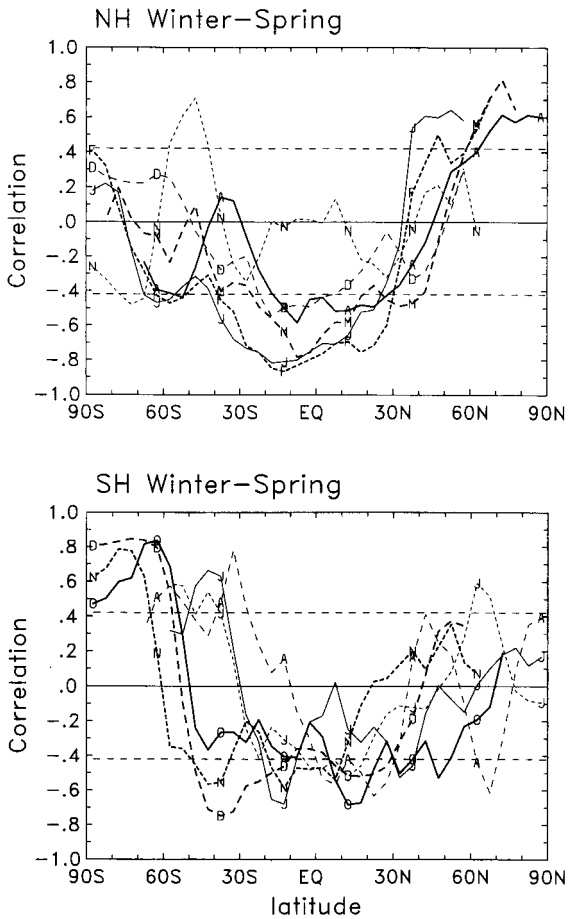


Fig. 6. Latitudinal structure of correlations between $\Delta O_3/\Delta t$ and $\overline{v'T'}$ for individual monthy calculations. Results in (a) show NH results for each month November–April (N = November, etc.), and (b) shows SH statistics for June–December. The horizontal dashed lines (at $\pm 0.42$) denote the 95% confidence level for these correlations.

2000), correlations which exceed 0.42 are significant at the 95% level. Results are shown for months when the wave activity is large, namely November–April in the NH (Fig. 6a) and June–December in the SH (Fig. 6b); note these are the time periods of positive $\Delta O_3/\Delta t$ in midlatitudes (Figs. 3–4). The observed correlations are weak in the NH during November–December, but become significant between January and April, during which time a latitudinal see-saw is evident (positive correlations in middle and high latitudes, and negative in the tropics). The region of positive correlations moves to polar latitudes in spring (March–April), so that ozone in midlatitudes only exhibits significant coherence during January–February. Figures 7–8 show example time series at several locations where the correlations are high: January over 40–50°N, and March over 60–90°N and 20°N-S. The January time series (Fig. 7) extends the 1979–1993 results shown in Fusco and Salby (1999). Note that while the correlations are highly significant (and remarkable), the amount of explained variance in $\Delta O_3/\Delta t$ ($r^2$) is still typically less than 0.5.

Strong negative correlations are observed in the tropics in Fig. 6a throughout winter and spring; the out-of-phase latitudinal behavior (compared to high latitudes) is a signature of fluctuations in the stratospheric Brewer-Dobson circulation. Figure 8b shows time series of tropical $\Delta O_3/\Delta t$ together with NH $\overline{v'T'}$ during March, showing this correlation. Comparisons with polar latitudes (Fig. 8a) show that the interannual changes in tropical and polar ozone tendencies are strongly anti-correlated

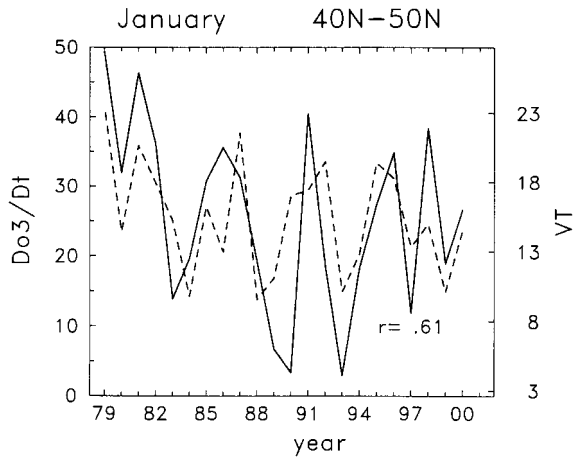


Fig. 7. Time series of $\Delta O_3/\Delta t$ (DU/month) over 40–50°N in January (solid line), together with January $\overline{v'T'}$ ($Kms^{-1}$—dashed line), for the period 1979–2000.

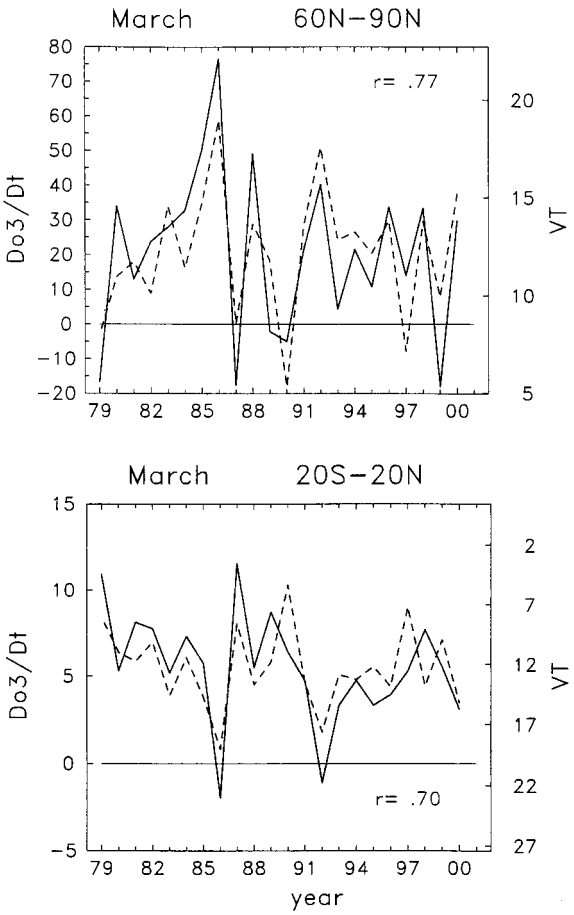


Fig. 8. Time series of $\Delta O_3/\Delta t$ (solid) and $\overline{v'T'}$ (dashed) for NH March statistics. Results are shown for the polar cap (60–90°N) in (a), and for the tropics (20°N-S) in (b); note the $\overline{v'T'}$ data are identical in (a)–(b), but the $\overline{v'T'}$ scale is inverted in (b).

(and coherent with the wave forcing), as shown previously in Fusco and Salby (1999).

Correlations between ozone tendency and $\overline{v'T'}$ in the SH are shown in Fig. 6b (here we have changed the sign of $\overline{v'T'}$, which is negative in the SH, because the expression for EP flux contains a Coriolis parameter term). The overall correlation patterns are very similar to those in the NH (Fig. 6a), namely: 1) positive correlations in extratropics and negative correlations in the tropics, and 2) a movement of the positive correlations from midlatitudes during winter (June–August) to the pole in spring (October–December). Figures 9–10 show time series over midlatitudes in June and over the polar cap in October, highlighting a remarkable coupling between the ozone tendency and dynamical forcing. October–November is the time of strong ozone increase following the Antarctic ozone hole conditions, which become established during September (e.g., Stolarski et al. 1986; Bevilacqua et al. 1997), but prior to vortex break-up (in November–December). The results in Fig. 10 show that the rate of increase during October is tightly coupled to the large-scale wave forcing from the troposphere.

The strong SH polar correlations extend to the time of vortex break-up and beyond, as shown for December results in Fig. 11. What is particularly interesting here is that the ozone tendency is tightly coupled to relatively small variability in $\overline{v'T'}$ ($\Delta O_3/\Delta t$ changes sign for modest changes in $\overline{v'T'}$ of only a few K-m/s). Additionally, there is a relatively strong trend in $\Delta O_3/\Delta t$ during the 1979–2000 period in Fig. 11, which is likely associated with systematic changes in the break-up date for the Antarctic vortex (Waugh et al. 1999). The sense of the trends is such that the later vortex break-up during the 1990's is correlated with enhanced planetary wave forcing in late spring (more negative $\overline{v'T'}$), plus enhanced persistence of the positive $\Delta O_3/\Delta t$ observed during October–November (see Fig. 2).

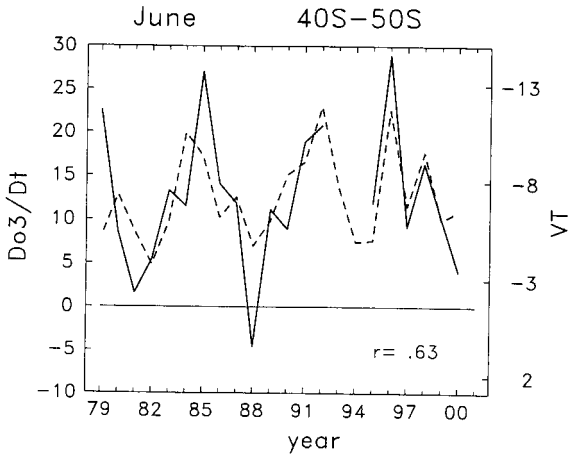


Fig. 9. Time series of $\Delta O_3/\Delta t$ over 40–50°S (solid) and $\overline{v'T'}$ (dashed) for SH statistics during June 1979–2000. Ozone data are unavailable for 1993–1994.

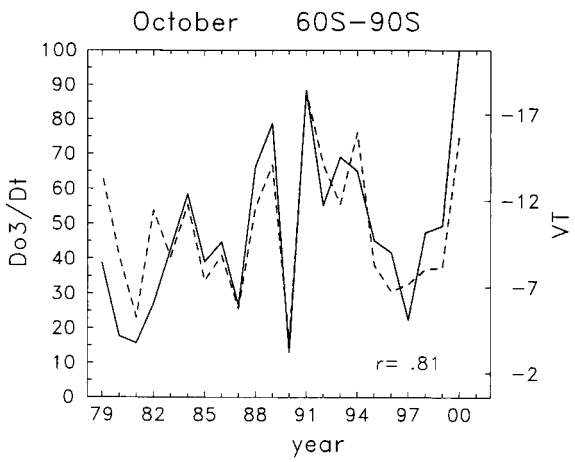


Fig. 10. Time series of $\Delta O_3/\Delta t$ over Antarctica (60–90°S) (solid) and $\overline{v'T'}$ (dashed) for SH October statistics during 1979–2000.

As a note, for the locations which exhibit a strong correlation between $\Delta O_3/\Delta t$ and $\overline{v'T'}$, it is possible to extend the relationship to estimate ozone tendencies in the absence of wave forcing (i.e., where $\overline{v'T'} = 0$). Comparison of this "zero wave forcing" ozone tendency to the actual observed tendencies then provides an empirical estimate of the net wave-driven circulation effects on column ozone. Results (not shown here) demonstrate that the large-scale

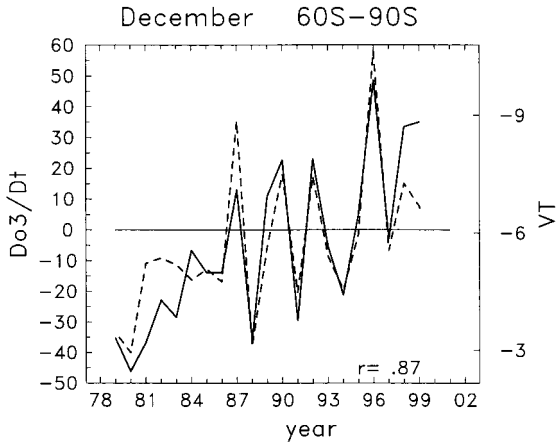


Fig. 11. Time series of $\Delta O_3/\Delta t$ over 60–90° (solid) and $\overline{v'T'}$ (dashed) for SH December statistics during 1979–1999.

circulation acts to reduce ozone in the tropics (at a rate of order −10 DU/month), and increase it during winter–spring over mid-latitudes (≈+30 DU/month) and over polar regions (rates up ≈+70 DU/month). These tropical decreases and extratropical increases are consistent with the conceptual model of global ozone transport by the Brewer-Dobson circulation.

## 5. Observed trends in planetary wave forcing

In Section 6 we will use the empirically-derived relationships between ozone change and wave forcing ($\overline{v'T'}$), together with observed variability in $\overline{v'T'}$, to estimate decadal trends in NH midlatitude ozone associated with long-term changes in $\overline{v'T'}$. As a prelude to those calculations, however, it is useful to examine the long-term variability (and trends) in observed $\overline{v'T'}$. As noted above, there are substantial uncertainties in estimates of $\overline{v'T'}$ and its variability, and we address this uncertainty by comparison of results based on three independent data sets: (1) NCEP reanalyses, (2) European Center for Medium Range Weather Forecasts (ECMWF) reanalyses (1979–1993) plus operational analyses (1994–2000), and (3) Climate Prediction Center (CPC) stratospheric analyses. Our analyses focus on both individual monthly means, plus the NH winter average November–March (which spans the active season, e.g., Fig. 3). We calculate trends using

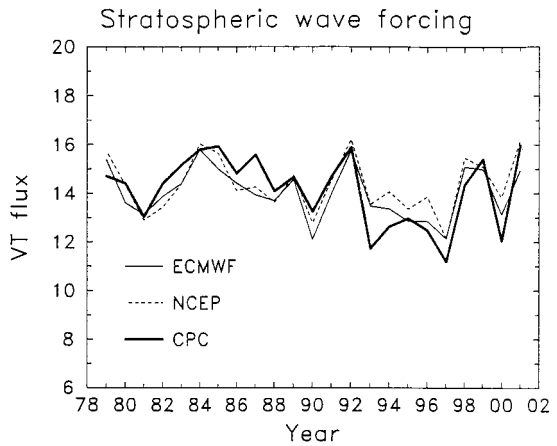


Fig. 12. Time series of seasonal average (November–March) NH $\overline{v'T'}$ during 1978–1979 to 2000–2001. Results are shown based on three different meteorological data sets, as discussed in text.

Table 1. Trends and one-sigma uncertainties in NH November–March average $\overline{v'T'}$. Units are K-m/s per decade.

| data source | time period | |
|---|---|---|
| | 1979-1992 | 1979-2000 |
| NCEP | 0.14 ± 0.73 | -0.26 ± 0.42 |
| ECMWF | -0.11 ± 0.74 | -0.45 ± 0.42 |
| CPC | 0.34 ± 0.61 | -1.0 ± 0.49 |

a standard regression model, assuming each year's data are independent.

Time series of the November–March average NH $\overline{v'T'}$ are shown in Fig. 12. There is a significant degree of interannual variability in these seasonal means, with values ranging from ~12–16 K-m/s. Overall there is reasonable agreement between the NCEP, ECMWF and CPC statistics for these seasonal means, with differences typically $\leq$1 K-m/s (i.e., somewhat less than the 'natural' variability). There is a relative maximum in wave forcing during the middle 1980's, and a relative minimum during the middle 1990's (accentuated in the CPC data), so that there is a slight negative trend for the overall 1979–2000 statistics. However, as tabulated in Table 1, the 1979–2000 linear trends are far from statistically significant based on the NCEP and ECMWF

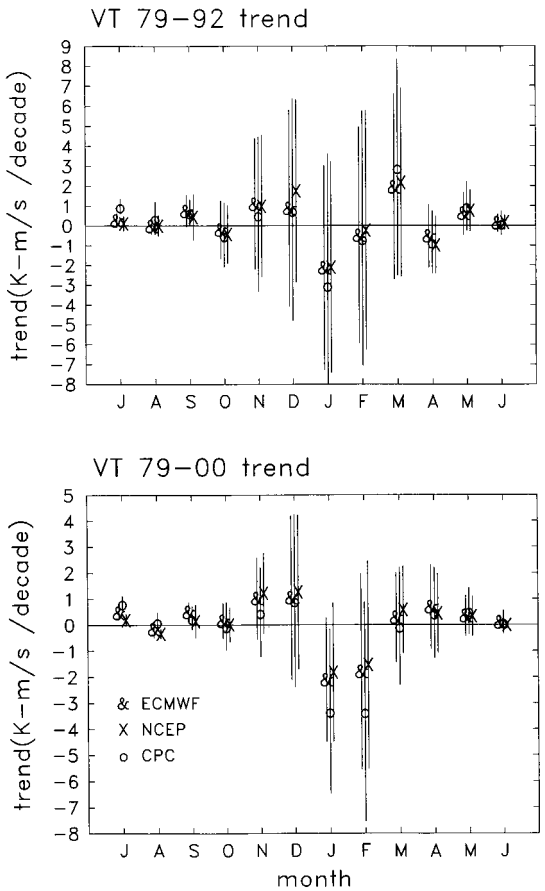


Fig. 13. Linear trends in monthly sampled NH $\overline{v'T'}$ statistics for each month of the year, calculated for the period 1979–1992 (top) and 1979–2000 (bottom). Results for each month are calculated based on three separate meteorological analyses. The error bars denote plus and minus two sigma uncertainty. Note the shift in axis to place NH winter in the middle of these plots.

data, due to the large 'natural' interannual variability in these statistics. The 1979–2000 trends based on the CPC data are just barely significant at the $2\sigma$ level.

Trends in NH $\overline{v'T'}$ for individual months are shown in Fig. 13 for two time periods (1979–1992, and 1979–2000), including results from all three data sources. For the 1979–1992 period, trends are highly variable during the winter and far from statistically significant during any month. For the longer 1979–2000 record, a more systematic pattern emerges of negative

trends during January–February, with weak positive trends during early winter (November–December). The negative trends during January are at the edge of ($2\sigma$) statistical significance, while those in February are less than significant. However, the overall seasonal pattern and magnitudes of trends are similar between the different data sets, suggesting an actual decrease in $\overline{v'T'}$ (in the face of considerable natural variability). We note that these results are consistent with Newman and Nash (2000), who report negative trends in NH $\overline{v'T'}$ for statistics covering January–February.

In summary, while winter averaged $\overline{v'T'}$ statistics do not exhibit statistically significant decadal trends, there have been decreases in NH $\overline{v'T'}$ during the months of January and February (for the longer 1979–2000 record). These January–February trends border on statistical significance (given a considerable amount of 'natural' interannual variability), but the consistency over two months (and agreement between different data sets) suggest an actual decrease during these midwinter months. Given the observed correlation between $\overline{v'T'}$ and polar stratospheric temperatures (Newman et al. 2001), we note that these midwinter decreases in $\overline{v'T'}$ are consistent with at least some portion of the contemporaneous cooling of the Arctic polar stratosphere in spring (Pawson and Naujokat 1999; Randel and Wu 1999; WMO 1999, Chapter 5). The degree to which these trends in $\overline{v'T'}$ influence midlatitude ozone are explored below.

## 6. Trends in NH midlatitude ozone related to planetary wave forcing

In this section we use the empirical correlations between $\Delta O_3/\Delta t$ and $\overline{v'T'}$ (Section 4), together with observed interannual variability of $\overline{v'T'}$ (Section 5), to estimate decadal-scale ozone changes associated with 'trends' in wave forcing. We focus here on ozone changes over NH midlatitudes during the months January–March, when the largest decadal trends are observed (Stolarski et al. 1991; WMO 1999). Our analyses involve two sets of calculations involving $\Delta O_3/\Delta t$ and $\overline{v'T'}$: (1) the ozone tendency is integrated in time to generate ozone time series (from which trends are calculated), and (2) step (1) is repeated, but using $\Delta O_3/\Delta t$ regressed upon $\overline{v'T'}$ to estimate the direct contribution of wave forcing. These calculations are explained in turn below.

As discussed above, there is a build-up of NH midlatitude column ozone during November–March of each year. There is substantial year-to-year variability in this build-up (some of which is related to the intensity of planetary wave forcing), but to a large degree the anomalies existing in late spring decrease during the summer, and ozone returns to approximately similar values by autumn of each year (Fusco and Salby 1999). Here we extend this empirical result by assuming that the ozone anomalies are identically zero at the beginning of each winter, and calculate ozone for each year by simply integrating $\Delta O_3/\Delta t$ during the winter–spring. Although the observed ozone tendencies are large during November–March (Fig. 3a), we integrate the tendencies only for the period of middle-late winter (January–March). This is because ozone is uncorrelated with $\overline{v'T'}$ during November–December (Fig. 6a), and our aim is to focus on planetary wave effects. Hence ozone for January, February and March of each year is given by:

$$O_3(t) = \int_{\text{January}}^{\text{March}} \frac{\Delta O_3}{\Delta t} \cdot dt. \qquad (1)$$

To reiterate, this calculation assumes that the ozone anomalies are identically zero at the beginning of January for each year (i.e., $O_3$ (January 1) = 0), and that any interannual or long-term changes arise due to variations after January 1. This is clearly an idealized assumption, but is implicit if changes in $\overline{v'T'}$ are a causal mechanism for interannual ozone change.

Figure 14 shows the interannual ozone anomalies at 50°N from the merged satellite data, together with the anomalies calculated from Eq. 1 (with data only for January–March of each year). This comparison gives a direct measure of the accuracy of assuming zero ozone anomalies on January 1 of each year (the curves would match identically if the observed January 1 anomalies were used instead). While there is approximate agreement in Fig. 14 for some years, there are also several years for which the correspondence is poor (the correlation between the data sets is 0.58 for the individual monthly means, and 0.60 for the Janu-

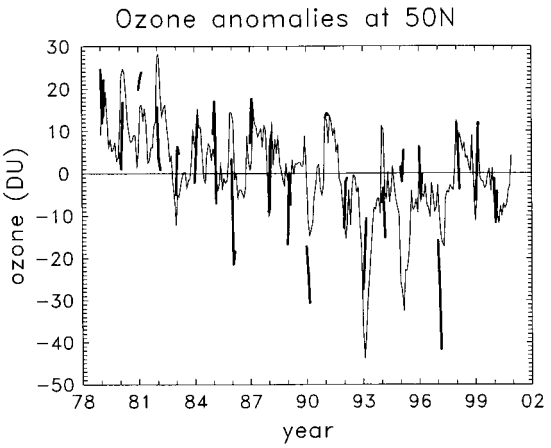


Fig. 14. The thin line shows the interannual anomalies in column ozone at 50°N from the merged satellite data set. The heavy lines show ozone anomalies calculated for January–March of each year, derived from Eq. 1 (assuming zero anomalies on January 1 of each year, and then integrating observed $\Delta O_3/\Delta t$).

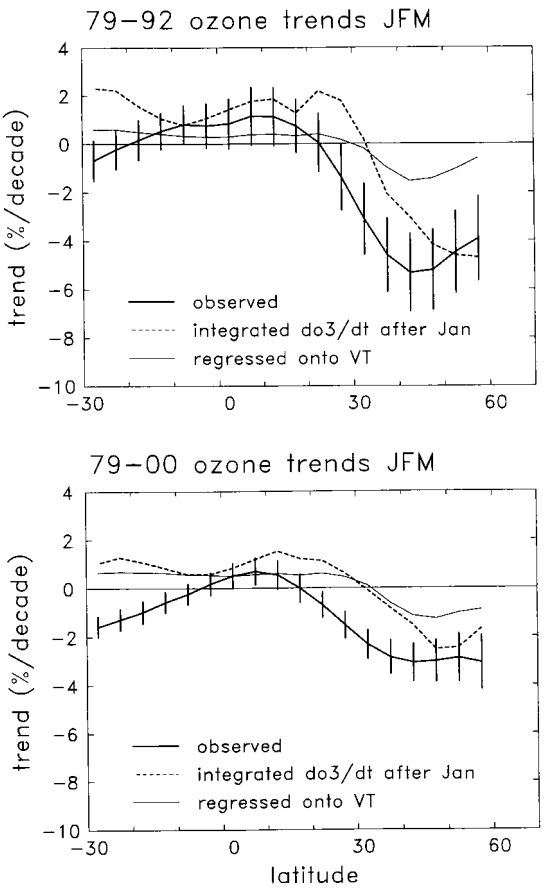


Fig. 15. Latitudinal profile of ozone trends during January–March for the period 1979–1992 (top) and 1979–2000 (bottom). The heavy lines show trends calculated from the merged satellite data, with two sigma statistical uncertainty levels. The dashed lines show trends calculated from the ozone resulting from Eq. 1 (assuming zero anomalies on January 1 of each year). The thin solid lines are ozone trends associated with changes in $\overline{v'T'}$, derived by regression. See text for details. Uncertainty levels are similar for all three calculations, but shown only for the observed trends.

ary–March averages). The lack of more detailed agreement in Fig. 14 demonstrates that ozone changes prior to January 1 can be a dominant effect in some years (and hence probably not directly related to anomalies in wave forcing).

In terms of decadal variability, there is some approximate agreement between the two time series in Fig. 14, with generally positive anomalies prior to ~1985, negative anomalies for several years during the middle 1990's, and near-zero values for 1998–2000. Figure 15a shows linear trends in January–March average ozone for the period 1979–1992, calculated from these two time series (i.e., the 'full' observed anomalies, and those calculated from Eq. 1). These trends were calculated using a standard regression model (e.g., Stolarski et al. 1991), and the period 1979–1992 is chosen for comparison to Fusco and Salby (1999) (the period 1979–2000 is considered below). The latitudinal structure of the observed ozone trends follows the familiar pattern of significant negative values over ~30–60°N, with insignificant (slightly positive) trends in the tropics. The trends calculated from Eq. 1 show a similar latitudinal structure, but shifted somewhat northward; there is poor agreement over latitudes ~25–35°N. However, these results show that a sizeable fraction of the observed trends over ~35–60°N occur due to anomalous tendencies after January 1, and the north-south see-saw patterns in ozone trends from Eq. 1 are

furthermore suggestive of a link to the large-scale circulation.

The explicit link between ozone trends and $\overline{v'T'}$ is made by integrating the ozone via Eq. 1, but instead of the 'full' $\Delta O_3/\Delta t$ we use the component linearly related to $\overline{v'T'}$, estimated via regression:

$$\frac{\Delta O_3}{\Delta t} = \alpha \cdot \overline{v'T'} + \text{residual}. \qquad (2)$$

The regression coefficient $\alpha$ is derived for each month (January–March) as a function of latitude (similar to the correlations in Fig. 5), and then values of $\Delta O_3/\Delta t$ are estimated from these $\alpha$ and the observed $\overline{v'T'}$. Trends are calculated from the resulting January–March ozone time series, and included in Fig. 15. The results for 1979–1992 show a latitudinal structure similar to the observed trends, but with a magnitude approximately ~20% of that observed over 35–60°N. This result is reasonable, given that (1) only a fraction of the trends arise from tendencies after January 1, and (2) only a fraction of $\Delta O_3/\Delta t$ is linearly related to $\overline{v'T'}$ during this time (Fig. 6a).

Figure 15b shows similar trend diagnostics calculated for the period 1979–2000. The latitudinal structure of the observed trends is similar to the 1979–1992 period, but with reduced magnitudes (due to the 'rebound' in ozone after ~1998 seen in Fig. 14). For the 1979–2000 period the January–March ozone trends directly related to $\overline{v'T'}$ have a magnitude of approximately −1% per decade over 35–60°N, and this is about 30% of the total trends over this latitude range. The slight fractional increase of the EP flux component over the 1979–1992 statistics is probably due to somewhat stronger $\overline{v'T'}$ trends during January–February for the 1979–2000 period (Fig. 13). However, the $\overline{v'T'}$ component is still a relatively small fraction of the total. Overall, these direct trend calculations suggest that approximately 20–30% of the observed NH midlatitude (35–60°N) ozone trends during the last two decades are directly attributable to changes in $\overline{v'T'}$.

Similar calculations of interannual variability in the SH are problematic because of uncertainties in the estimated EP fluxes. Figure 16 shows time series of deseasonalized anomalies in $\overline{v'T'}$ for both the NH and SH (over 40–70°N and 40–70°S), comparing statistics derived from NCEP reanalyses with those from ECMWF (a combination of reanalyses over 1979–1993, plus operational analyses for 1994–2000). The comparisons in Fig. 16 show excellent agreement in the NH (rms differences of ~10%), but significant differences in the SH. These uncertainties in derived eddy fluxes are probably related to the lack of a dense radiosonde network in the midlatitudes SH. Furthermore, the NCEP data show a decadal-scale trend in SH EP fluxes (increase in $\overline{v'T'}$ between the 1980's and 1990's), whereas the ECMWF statistics do not. These different low frequency variations in NCEP or ECMWF $\overline{v'T'}$ SH statistics result in significantly different estimated dynamical trends in ozone. Because of these uncertainties, reliable estimates of decadal-scale dynamical changes in the SH are not possible at present.

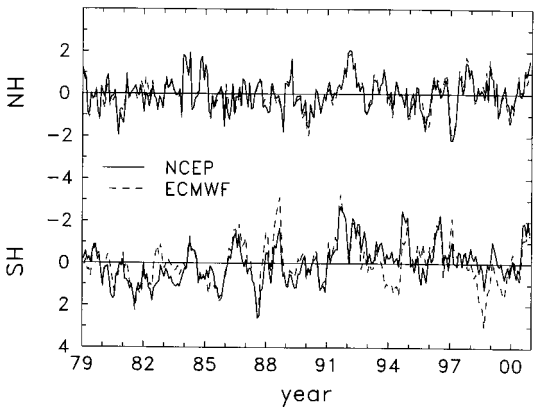


Fig. 16. Time series of deseasonalized interannual anomalies in $\overline{v'T'}$ ($\mathrm{Kms}^{-1}$) in the NH (top) and SH (bottom), based on statistics derived from the NCEP/NCAR reanalyses (solid lines) and ECMWF reanalyses and operational data (dashed lines). Note the inverted scale for the SH statistics; negative values correspond to stronger $\overline{v'T'}$. Overall there is good agreement in the NH, but significant differences in the SH.

## 7. Summary and discussion

We have used a long observational record (1979–2000) to quantify the monthly and latitudinal patterns of correlation between column

ozone tendency and the EP flux entering the lower stratosphere. While column ozone is expected to respond to dynamical variability over a range of altitudes, there are remarkably strong correlations found using a single dynamical proxy as a measure of the large scale stratospheric circulation ($\overline{v'T'}$ at 100 mb). The overall patterns of correlation between $\overline{v'T'}$ and $\Delta O_3/\Delta t$ are similar between hemispheres, showing: 1) a latitudinal see-saw, with negative correlations in the tropics and positive values in high latitudes, and 2) a movement of the positive correlations to polar latitudes in spring. Somewhat surprising is the lack of strong correlations in the NH mid latitudes during autumn (November–December), when strong positive ozone tendencies are thought to result from wave-driven transport effects.

The strong correlations observed in polar regions (Figs. 8a and 10) demonstrate that large-scale circulation effects are a primary factor in polar ozone change during spring (unfortunately the TOMS/SBUV data do not allow polar analyses during midwinter). Changes in Arctic ozone during spring (March–April) are highly correlated with wave forcing, and furthermore the rate of recovery of the Antarctic ozone hole during October–November is strongly modulated by dynamics. These polar correlations extend well into late spring-early summer (May in the NH and January in the SH). The overall sensitivity of polar ozone to relatively small changes in wave driving is remarkable (for example, see Fig. 11); this is likely related to geometry of the converging Brewer-Dobson circulation over the pole. Note that the relationship to circulation effects quantified here does not minimize the importance of springtime polar chemistry, which is known to contribute substantial (additional) interannual variability (e.g., Chipperfield and Pyle 1998). Photochemical relaxation is a further source of variance in $\Delta O_3/\Delta t$ during spring and summer, as evidenced by anticorrelation with ozone itself (Fig. 5).

We have furthermore used the observed correlations between ozone tendency and $\overline{v'T'}$, together with observed interannual variations in $\overline{v'T'}$, to directly estimate components of ozone 'trends' attributable to long-term changes in wave forcing. Observed trends in NH wave forcing ($\overline{v'T'}$) show small and insignificant changes for the period 1979–1992, but for the longer period 1979–2000 there are systematic decreases during January and February, which border on statistical significance. The calculations here suggest that these interannual changes in stratospheric wave forcing are associated with relatively modest decadal-scale ozone changes, (column ozone trends of order $-1\%$ per decade). Direct calculation of the ozone trends during the period 1979–1992 shows that wave forcing accounts for $\sim 20\%$ of the observed trends over 35–60°N, while for the longer record 1979–2000 the fraction is slightly larger ($\sim 30\%$). The significant ozone trends evident over $\sim$25–35°N do not have an important contribution related to the EP flux. Thus the direct effects of EP flux changes on decadal ozone trends appears limited to $\sim$20–30% over middle to high latitudes, and less on a hemispheric average.

## Acknowledgments

This work was partially supported under NASA Grants W-18181 and W-16215, under the ACMAP and UARS Guest Investigator programs. We thank Andy Dessler, Andrew Fusco, Rolando Garcia, Roland Madden, Jim Miller, Paul Newman, Murry Salby, Anne Smith and two anonymous referees for discussions and constructive reviews. Marilena Stone expertly prepared the manuscript. The National Center for Atmospheric Research is operated by the University Corporation for Atmospheric Research under the sponsorship of the National Science Foundation.

## References

Allaart, M.A.F., H. Kelder and L.C. Heijboer, 1993: On the relation between ozone and potential vorticity. *Geophys. Res. Lett.*, **20**, 811–814.

Andrews, D.G., J.R. Holton and C.B. Leovy, 1987: *Middle Atmosphere Dynamics*. Academic Press, 489 pp.

Bevilacqua, R.M., et al., 1997: POAM II observations of the Antarctic ozone hole in 1994, 1995 and 1996. *J. Geophys. Res.*, **102**, 23643–23657.

Chipperfield, M.P. and J.A. Pyle, 1998: Model sensitivity studies of Arctic ozone depletion. *J. Geophys. Res.*, **103**, 28389–28403.

Fritz, S. and D. Soules, 1972: Planetary variations of stratospheric temperature. *Mon. Wea. Rev.*, **100**, 582–589.

Fusco, A.C. and M.L. Salby, 1999: Interannual variations of total ozone and their relationship to variations of planetary wave activity. *J. Climate*, **12**, 1619–1629.

Garcia, R.R., 1987: On the mean meridional circulation of the middle atmosphere. *J. Atmos. Sci.*, **44**, 3599–3609.

Hadjinicolaou, P., A. Jrrar, J.A. Pyle and L. Bishop, 2002: The dynamically driven long-term trend in stratospheric ozone over northern middle latitudes. *Quart. J. Roy. Meteor. Soc.*, in press.

———, J.A. Pyle, M.P. Chippenfield and J.A. Kettleborough, 1997: Effects of interannual meteorological variability on middle latitude ozone. *Geophys. Res. Lett.*, **24**, 2993–2996.

Haynes, P.H., C.J. Marks, M.E. McIntyre, T.G. Shepherd and K.P. Shine, 1991: The "downward control" of extratropical diabatic circulations by eddy-induced mean zonal forces. *J. Atmos. Sci.*, **48**, 651–678.

Hood, L., S. Rossi and M. Beuten, 1999: Trends in lower stratospheric zonal winds, Rossby wave breaking behavior, and column ozone at northern midlatitudes. *J. Geophys. Res.*, **104**, 24321–24339.

Kalnay, E., et al., 1996: The NCEP/NCAR 40-year reanalysis project. *Bull. Amer. Meteor. Soc.*, **77**, 437–471.

Kinnersley, J.J. and K.K. Tung, 1998: Modeling the global interannual variability of ozone due to the equatorial QBO and to extratropical planetary wave variability. *J. Atmos. Sci.*, **55**, 1417–1428.

Mahlman, J.D., H. Levy and W.J. Moxim, 1986: Three-dimensional simulations of stratospheric $N_2O$: Predictions for other trace constituents. *J. Geophys. Res.*, **91**, 2687–2707.

Newman, P.A. and E.R. Nash, 2000: Quantifying the wave driving of the stratosphere. *J. Geophys. Res.*, **105**, 12485–12497.

———, ——— and J.E. Rosenfield, 2001: What controls the temperature of the Arctic stratosphere during the spring? *J. Geophys. Res.*, **106**, 19999–20010.

Pawson, S. and B. Naujokat, 1999: The cold winters of the middle 1990's in the northern lower stratosphere. *J. Geophys. Res.*, **104**, 14209–14222.

Randel, W.J., 1993: Global variations of zonal mean ozone during stratospheric warming events. *J. Atmos. Sci.*, **50**, 3308–331.

——— and J.B. Cobb, 1994: Coherent variations of monthly mean total ozone and lower stratospheric temperature. *J. Geophys. Res.*, **99**, 5433–5447.

———, et al., 1994: Simulation of stratospheric $N_2O$ in the NCAR CCM2: Comparisons with CLAES data and global budget analyses. *J. Atmos. Sci.*, **51**, 2834–2845.

——— and F. Wu, 1999: Cooling of the Arctic and Antarctic polar stratospheres due to ozone depletion. *J. Climate*, **12**, 1467–1479.

Schubert, S.D. and M.J. Munteanu, 1988: An analysis of tropopause pressure and total ozone correlations. *Mon. Wea. Rev.*, **116**, 569–582.

Smith, A.K., 1995: Numerical simulation of global variations of temperature, ozone and trace species in the stratosphere. *J. Geophys. Res.*, **100**, 1253–1269.

Steinbrecht, W., et al., 1998: Correlations between tropopause height and total ozone: Implications for long term changes. *J. Geophys. Res.*, **103**, 19183–19192.

Stolarski, R.S., A.J. Kreuger, M.R. Schoeberl, R.D. McPeters, P.A. Newman and J.C. Alpert, 1986: NIMBUS 7 satellite measurements of the springtime Antarctic ozone decrease. *Nature*, **332**, 808–811.

———, P. Bloomfield, R.D. McPeters and J.R. Herman, 1991: Total ozone trends deduced from Nimbus 7 TOMS data. *Geophys. Res. Lett.*, **18**, 1015–1018.

———, S. Hollandsworth, R. McPeters, L. Flynn and G. Labow, 2002: A 20-year data set for total column ozone derived from multiple satellite instruments. *J. Geophys. Res.*, in preparation.

Waugh, D.W., W.J. Randel, S. Pawson, P.A. Newman and E.R. Nash, 1999: Persistence of the lower stratosphere polar vortices. *J. Geophys. Res.*, **104**, 27191–27202.

World Meteorological Organization (WMO), 1999: Scientific Assessment of Ozone Depletion: 1998. WMO Rep. No. 44.

Ziemke, J.R., S. Chandra, R.D. McPeters and P.A. Newman, 1997: Dynamical proxies of column ozone with applications to global trend models. *J. Geophys. Res.*, **102**, 6117–6129.